16. Homonuclear Correlated spectroscopy (COSY)

Homonuclear Correlated spectroscopy (COSY) was the first 2D experiment introduced. Jeener[2] proposed the experiment in 1971 and Aue, Barthodi, and Ernst[3] analyzed and experimentally demonstrated the technique in their seminal paper in 1976. Several modifications to COSY quickly followed and the experiment was applied to many systems.

16.1 COSY

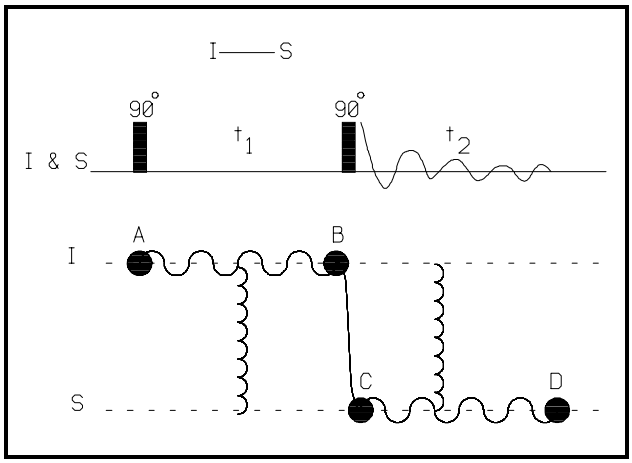

Figure 16.1.1. COSY pulse sequence and CFN diagram.

The COSY pulse sequence consists of two pulses separated by an incremented t_1 delay. The spins are allowed to come to thermal equilibrium (or a steady state) before applying the first 90° pulse, which generates transverse magnetization at <A> in the COSY CFN (Figure 6.1.1). During <A,B>, spin **I** precesses at the **I** spin frequency and simultaneously evolves via coupling into antiphase $\mathbf{2I_xS_z}$ at <B>. Coherence transfer from **I** to **S**, <B,C>, is effected by the second 90° pulse on both spins. The **S** spin then evolves under both **S** chemical shift and coupling to **I** during detection, <C,D>.

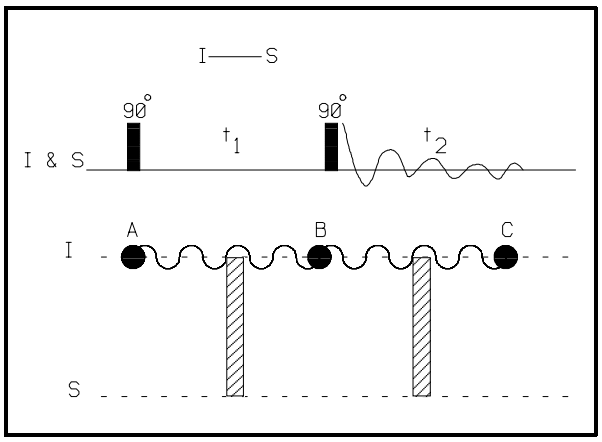

Figure 16.1.2. CFN for COSY diagonal peaks.

Cross peaks in COSY appear at the intersection of the frequencies of the scalar coupled spins. In this example, a cross peak would occur at the **I** spin frequency along $\omega_1^{\mathbf{I}}$ and at the S spin frequency along $\omega_2^{\mathbf{S}}$, ($\omega_1^{\mathbf{I}}$,$\omega_2^{\mathbf{S}}$). Since the **S** spin also serves as a source of magnetization, there will also be a cross peak representing **S** coherence that is transferred to **I** coherence at ($\omega_1^{\mathbf{S}}$,$\omega_2^{\mathbf{I}}$). The active coupling that occurs during <A,B> and <C,D> gives rise to multiplet peaks that are antiphase (See Figure 16.2.1).

Diagonal peaks in a COSY spectrum arise from magnetization that remains on the same spin after the second 90° pulse.

The frequencies are identical for both t_1 and t_2 periods and peaks are found at (ω_1^I,ω_2^I) and (ω_1^S,ω_2^S). Figure 16.1.2 contains the CFN for the diagonal peaks of the COSY spectrum. Note that, unlike the case for the cross peaks, there is only passive coupling during both t_1 and t_2. Passive coupling results in multiplet peaks being inphase in the final spectrum. The CFN does not explicitly indicate the relative phase of the cross and diagonal peaks; below the detailed analysis shows that the cross peaks and diagonal peaks are 90° out of phase (See Figure 16.2.2).

Preparation:

$$\mathbf{I}_z = \pi/2\hat{\mathbf{I}}_x \Rightarrow -\mathbf{I}_y \qquad (16.1.1)$$

Evolution (t_1):

$$= \omega_I t_1 \hat{\mathbf{I}}_z \Rightarrow -\mathbf{I}_y \cos \omega_I t_1 + \mathbf{I}_x \sin \omega_I t_1 \qquad (16.1.2)$$

$$= \pi J_{IS} t_1 \mathbf{2}\hat{\mathbf{I}}_z\hat{\mathbf{S}}_z \Rightarrow (-\mathbf{I}_y \cos \pi J_{IS} t_1 + \mathbf{2I}_x\mathbf{S}_z \sin \pi J_{IS} t_1) \cos \omega_I t_1 + (\mathbf{I}_x \cos \pi J_{IS} t_1 + \mathbf{2I}_y\mathbf{S}_z \sin \pi J_{IS} t_1) \sin \omega_I t_1 \qquad (16.1.3)$$

Mixing:

$$= \pi/2(\hat{\mathbf{I}}_x+\hat{\mathbf{S}}_x) \Rightarrow (-\mathbf{I}_z \cos \pi J_{IS} t_1 - \mathbf{2I}_x\mathbf{S}_y \sin \pi J_{IS} t_1) \cos \omega_I t_1 + (\mathbf{I}_x \cos \pi J_{IS} t_1 - \mathbf{2I}_z\mathbf{S}_y \sin \pi J_{IS} t_1) \sin \omega_I t_1 \qquad (16.1.4)$$

During the detection period, t_2, the spin system evolves under chemical shift and coupling operators. The receiver is turned on and the signals are detected.
If all of the terms are retained, the calculation becomes very cumbersome due to the large number of terms that are generated. A great simplification of the product operator calculations is achieved by only calculating the evolution of the observable signals during the detection period. Only $\mathbf{I}_x$, $\mathbf{I}_y$, $\mathbf{S}_x$, and $\mathbf{S}_y$ give directly observable signals in the NMR spectrometer. The pertinent terms at the beginning of the detection period are the direct observables and any terms that will evolve into observables due to coupling (*e.g.,* $\mathbf{2I}_z\mathbf{S}_y$). All other coherences are not observable. During the detection period of the COSY experiment there are 13 terms that evolve. All of the directly observable terms arise from the $\mathbf{I}_x$ and $\mathbf{2I}_z\mathbf{S}_y$ terms created during the mixing period. The $\mathbf{I}_x$ term evolves by chemical shift into $\mathbf{I}_y$, and the $\mathbf{2I}_z\mathbf{S}_y$ term evolves through coupling into $\mathbf{S}_x$ that further evolves into $\mathbf{S}_y$ by chemical shift. The interesting terms present at the beginning of the detection period are:

$$\mathbf{I}_x \cos \pi J_{IS} t_1 \sin \omega_I t_1 \qquad (16.1.5)$$

and

$$-\mathbf{2I}_z\mathbf{S}_y \sin \pi J_{IS} t_1 \sin \omega_I t_1 \qquad (16.1.6)$$

These signals will further evolve under J_{IS} coupling and chemical shift during t_2 into

$$\mathbf{I}_x \exp(i\,\omega_I t_2) \cos \pi J_{IS} t_2 \cos \pi J_{IS} t_1 \sin \omega_I t_1 \qquad (16.1.7)$$

and

$$\mathbf{S}_x \exp(i\,\omega_S t_2) \sin \pi J_{IS} t_2 \sin \pi J_{IS} t_1 \sin \omega_I t_1. \qquad (16.1.8)$$

16.2 Interpretation of COSY spectra

The signals that have the frequency of the **I** spin during both t_1 and t_2 are diagonal peaks (Eqn.16.1.5). The **S** signals, which precess at the **S** frequency during t_2, are frequency labeled during t_1 with the frequency of the **I** spin; these are the cross peaks (Eqn.16.1.6). There are two significant features of these different signals: 1). the coupling modulation of the cross peak signals in both t_1 and t_2 is a sine function, whereas for the diagonal peaks the modulation is a cosine function; and 2). there is a 90° phase difference between the $-\mathbf{I}_y$ and $2\mathbf{I}_z\mathbf{S}_x$ terms at the beginning of the acquisition (Eqns.16.1.5 and16.1.6). The first feature means that the cross peak multiplets are antiphase in both dimensions (Figure16.2.1) whereas the diagonal multiplets are inphase is both dimensions (Figure16.2.2.). The second feature means that when the cross-peaks are phased to absorption mode, as in Figure16.2.1, then the diagonal peaks have a dispersive line shape shown in Figure16.2.2. The dispersive nature of the diagonal peaks cause perturbations over a wide area around the peaks. Notice the extent of the baseline distortions around the diagonal peaks (Figure16.2.1) as compared to the flat baseline around the cross peak in (Figure16.2.2). For peaks with linewidths on the order of the coupling constant, the positive part of the antiphase line partially cancels the negative part reducing the intensity of the cross peak. The diagonal peaks, on the other hand, are inphase and the multiplets constructively interfere. This combined with the fact that the diagonal peaks are phased to a dispersive lineshape, makes the diagonal peaks large. Cross peaks of coupled spins having similar chemical shifts are close to the diagonal and are difficult to observe since they are swamped by the large diagonal peaks. The combination of these features creates undesirable spectral characteristics in the COSY spectrum. Application of a

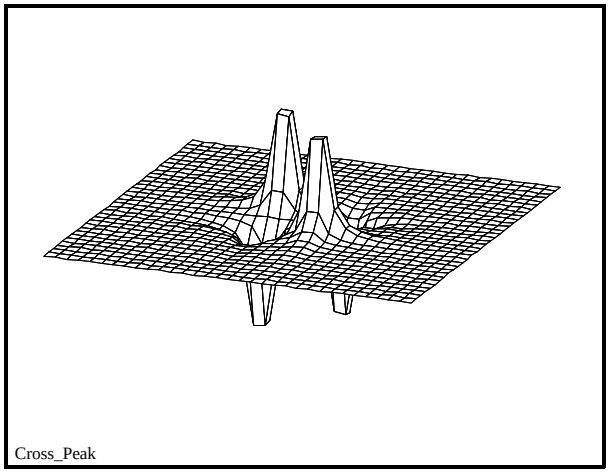

Figure16.2.1. Simulated antiphase, absorptive COSY-type cross peak. The linewidth used in the simulation was 10% of the coupling constant.

heavy filter function (*e.g.* unshifted sinebell) reduces the diagonal amplitude with respect to the cross peaks while distorting the lineshape. Mueller[1] has used a time domain convolution difference filter to reduce the diagonal peaks of a COSY spectrum with little disturbance of cross peaks.

A common misconception held by novices is that the cancellation of cross peaks due to linewidths that are of the same order or larger than the coupling constant can be overcome by using the "magnitude" mode instead of the "phase sensitive" mode of collecting COSY data. The confusion comes from the differences in the appearance of the spectra obtained by the two methods. Peaks in magnitude mode spectra have only positive peaks since during *processing* the square root of the sum of the squares (the magnitude) of the absorption and corresponding dispersion peaks is obtained. Since it appears that all of the cross peak components have the same algebraic sign, they **apparently** do not cancel as they would in a phase sensitive spectrum where the spectrum is displayed as positive and negative absorption mode peaks. However, the sensitivity of the phase sensitive spectra is theoretically greater than that of the magnitude spectrum by a square root of two. The reason that the magnitude calculation is performed in magnitude mode spectra is that the inherent lineshape of the cross peaks is phase twisted, *i.e.* the peaks contain an inseparable mixture of both *antiphase* absorptive and *antiphase* dispersive line shapes. The resolution afforded by phase-twisted line shapes is not as good as that of the pure absorption line shape. The data processing of the magnitude applies a sinebell or other digital filter that induces approximate symmetry on the time domain data. Fourier Transform of the data followed by a magnitude calculation gives approximately absorptive lineshapes while throwing away the phase information. Any cancellation in the cross peak has already occurred during the generation of the antiphase state when the data was collected. The extra square-root-of-two sensitivity in the phase sensitive spectrum comes from the additional coherence transfer pathway that is allowed by the phase cycling.

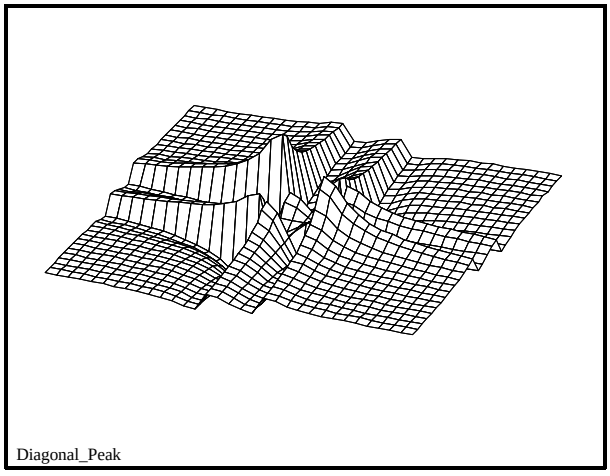

Figure16.2.2. Simulated diagonal peak from a COSY experiment. The linewidth to coupling constant ratio was the same as in Figure16.2.2.

16.3 COSY phase cycling:

COrrelation SpectroscopY (COSY):

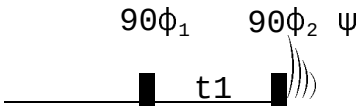

COSY Coherence Transfer Pathway:

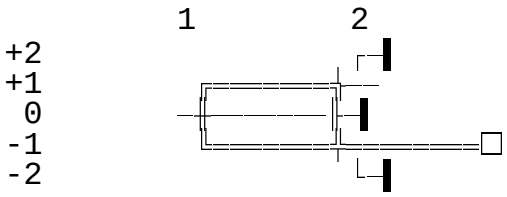

The first pulse excites longitudinal to transverse magnetization. The desired coherence order changes are then

$\Delta m_1 = \pm 1$

The second pulse is the mixing pulse; all possible coherence order changes can occur. The desired changes are those that cause transfer from +1 => -1 coherence and -1 => -1 coherence (Eqn.16.1.4), specifically,

$\mathbf{2I_yS_z} \Rightarrow \mathbf{2I_zS_y}$

and

$\mathbf{I_x} \Rightarrow \mathbf{I_x}$

These changes represent transfers of $\Delta m_2 = 0,-2$.

Following the rules for phase cycling (Section 3.6), we obtain the phase cycles for ϕ_1, ϕ_2, and ψ.

ϕ_1:
+1 (0 **-1**)
N=2
$\phi_1 = 2\pi k/2 \quad k=0,1$
$\phi_1 = 0,\pi$

ϕ_2:
+3 **+2** +1 **0** (-1 **-2**) -3
N=2
$\phi_2 = 2\pi k/2 \quad k=0,1$
$\phi_2 = 0,\pi$

Note that for ϕ_2 both $\Delta m=0$ and +2 are in bold. These order changes are also allowed, as are all order changes for $\Delta m = \Delta m_{sel} \pm n*N$ with n an integer.
For the receiver phase:

$\psi = 0,\pi,0,\pi$

e.g. For step 4 in the table below, the receiver phase is calculated for the -1,0 pathway as:

$\psi_4 = -[(-1)(\pi) + (0)(\pi)] = \pi$

or for +1, -2 pathway

$\psi_4 = -[(+1)(\pi) + (-2)(\pi)] = \pi$

This leads to a very simple phase table for COSY experiment.

$\phi_1 = 2(0\ \pi)$
$\phi_2 = 2(0)\ 2(\pi)$
$\psi\ = 2(0\ \pi)$

Since this phase cycle permits $\Delta m=+2$ transfer at the second pulse, the resulting -1 => +1 transfer can lead to quadrature images. To restrict the CTP further one can force the coherence to start at level 0 and end at level -1. In this CTP, the entire COSY pulse sequence is used as a black box that generates $\Delta m = -1$ transfer from thermal equilibrium. The equivalent overall CTP is:

Analyzing this overall CTP we obtain

ϕ_c:

Δm_1=-1
(**-1** 0 1)
N=3
ϕ_c = 0,2π/3,4π/3

This CTP leads to 120° phase shifts, which are not available on all spectrometers. It is always permitted to eliminate coherence pathways that do not exist, so to use 90° phase shifts, available on most spectrometers, we add a fictitious transfer of $+\Delta 2$ from the 0 level. Note that from thermal equilibrium this is a forbidden transition.

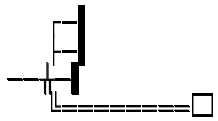

Again we calculate the phase cycle

ϕ_c:

Δm_1=-1

(**-1** 0 1 2)
N=4
ϕ_c = 0,π/2,π,3π/2

These are the more common 90° degree phase shifts.

We can generate a new phase table for the overall sequence. These phases, ϕ_c, are to be applied to **all** of the pulses and receiver simultaneously.

ϕ_c = 0 π/2 π 3π/2
ψ = 0 π/2 π 3π/2

This phase cycle is added "on top" of the other phase cycle to give the final table consisting of 16 steps.

ϕ_1 = 2(0 π) 2(π/2 3π/2) 2(π 0) 2(3π/2 π/2)
ϕ_2 = 2(0) 2(π) 2(π/2) 2(3π/2) 2(π) 2(0) 2(3π/2) 2(π/2)
ψ = 2(0 π) 2(π/2 3π/2) 2(π 0) 2(3π/2 π/2)

16.4 Variants of COSY

Coherence transfer in COSY occurs through an antiphase state at state <B> (Figure 16.1.1). If the <A,B> evolution period is short compared to 1/(2J) then very little coherence is transferred and the resulting cross peaks are weak. In experiments that are collected rapidly, the limiting time is the number of points that are collected along t_1. Obviously, the number of t_1 points must be kept small in order to keep the experimental time short. In the original COSY experiment, this would yield very little antiphase coherence at state <B>, and therefore, very weak cross peaks would result. An alternative is to use a constant time for the t_1 period[2]. This consists of the <A,B> period being set to a fixed time, *e.g.* 1/(2J), and a 180° pulse systematically moved within this period to generate the t_1 evolution period. When the 180° pulse is centered, there is no chemical shift evolution; however, since the 180° pulse is non-selective, coupling will proceed throughout the entire constant time period (Table 2.1B). As the 180° pulse is moved from the center there will be an increasing amount of chemical shift precession and frequency labeling of the coherence. In the constant time experiment, the amount of antiphase coherence at <B> is constant. Since there is no time dependent modulation of the **I** coherence by coupling, the peaks along ω_1 will be singlets (decoupled from all other spins).

In situations where the transverse decay rate is fast compared to the reciprocal of the coupling constant, *i.e.* broad lines, the usable t_1 period is limited, and therefore, the cross peaks are weak. Line broadening can arise from a variety of sources including chemical exchange or lifetime broadening, paramagnetic broadening, or strong dipolar interactions due to long correlation times. With infinite sensitivity this does not cause a problem, but realistically, once the line width becomes a few times

larger than the coupling constant the cross peaks become vanishingly small. The linewidth of protons in macromolecules becomes a limiting factor for COSY experiments at about 20,000 daltons. Above this molecular weight, the cross peaks are difficult to observe at typical concentrations of 1-10 mM.

16.5 Multiple Quantum Filtered Spectroscopy

Multiple quantum filtration of correlation spectra allows the scientist to use the topologies of the scalar coupling network to unravel the complexities of the spin system under study. Multiple quantum effects were known long before the introduction of 2D spectroscopy, but the production and interpretation of these effects were difficult. Using hard pulses on non-equilibrium states of the density matrix, in general, produces coherences that can have more than one transverse component. These coherences evolve under a Hamiltonian that has contributions from all spins involved in the coherence. It is this property that can be exploited for the study of complex spin systems.

16.5.1 Double Quantum Filtered COSY (DQFCOSY)

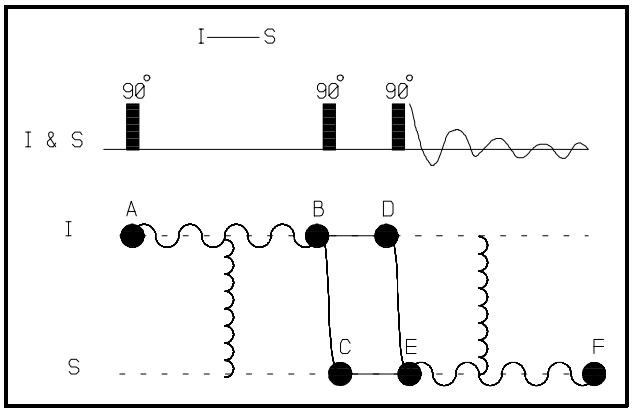

16.4.1. CFN for Double Quantum Filtered COSY.

Double quantum filtered COSY reduces the problem of the dispersive diagonal peak that exists in COSY spectra.[3] Figure 16.5.1 shows a DQFCOSY pulse sequence and its associated CFN. The spins are allowed to come to thermal equilibrium or a steady state at <A>. The first 90° pulse generates transverse magnetization. During <A,B> the spin precesses at its chemical shift frequency and simultaneously evolves via coupling into an antiphase state at <B>. The second 90° pulse generates, among others, a double quantum coherence designated by the simultaneous transverse lines <B,D> and <C,E> for the **I** and **S** spins. The time period for <B,D> (and <C,E>) is kept short to eliminate any chemical shift precession at the double quantum frequency. The final pulse recovers antiphase coherence from the double quantum state at <E>. The $\mathbf{I_zS^{\pm}}$ antiphase coherence precesses at the chemical shift frequency of **S** and refocuses into observable, inphase magnetization during the acquisition time, <E,F>.

The main difference between this sequence and the COSY sequence is that after the second 90° pulse in DQFCOSY the double quantum coherence is selected whereas in COSY the single quantum coherence is selected and detected. The double quantum coherence at <B,D><C,E> is not directly observable and the final pulse is used to regenerate single quantum coherence. The selection of the double or single quantum coherence is accomplished by the particular phase cycle of the pulse sequence.

16.5.2 Product operator description of the DQFCOSY

Preparation:

$$\mathbf{I}_z \;=\pi/2\hat{\mathbf{I}}_x\Rightarrow -\mathbf{I}_y \qquad (16.5.1)$$

Evolution due to chemical shift:

$$-\mathbf{I}_y \quad =\omega_I t\hat{\mathbf{I}}_z\Rightarrow \quad -\mathbf{I}_y \cos\omega_I t_1 + \mathbf{I}_x \sin\omega_I t_1 \qquad (16.5.2)$$

Evolution due to coupling:

$$=\pi J_{IS} t 2\hat{\mathbf{I}}_z\hat{\mathbf{S}}_z\Rightarrow \quad \begin{aligned}&(-\mathbf{I}_y \cos\pi J_{IS}t_1 + 2\mathbf{I}_x\mathbf{S}_z \sin\pi J_{IS}t_1) \cos\omega_I t_1 \\ &+ (\mathbf{I}_x \cos\pi J_{IS}t_1 + 2\mathbf{I}_y\mathbf{S}_z \sin\pi J_{IS}t_1) \sin\omega_I t_1\end{aligned} \qquad (16.5.3)$$

First mixing pulse:

$$=\pi/2(\hat{\mathbf{I}}_x+\hat{\mathbf{S}}_x)\Rightarrow \quad \begin{aligned}&(-\mathbf{I}_z \cos\pi J_{IS}t_1 - 2\mathbf{I}_x\mathbf{S}_y \sin\pi J_{IS}t_1) \cos\omega_I t_1 \\ &+ (\mathbf{I}_x \cos\pi J_{IS}t_1 - 2\mathbf{I}_z\mathbf{S}_y \sin\pi J_{IS}t_1) \sin\omega_I t_1\end{aligned} \qquad (16.5.4)$$

We can simplify the analysis at this point by applying a double quantum filter. A rudimentary double quantum filter can be implemented by subtracting this result (Eqn. 16.5.4) from a result where the first two pulses are shifted in phase by 90°. The phase shift substitutes $2\mathbf{I}_y\mathbf{S}_x$ for the $2\mathbf{I}_x\mathbf{S}_y$ term in Eqn. 16.5.4. The action of the filter is to retain only the term $2\mathbf{I}_x\mathbf{S}_y$ in the first phase cycle step and the $2\mathbf{I}_y\mathbf{S}_x$ term from the second step of the phase cycle. Individually, the $2\mathbf{I}_x\mathbf{S}_y$ and $2\mathbf{I}_y\mathbf{S}_x$ terms are superpositions of zero and double quantum coherence. This can be seen from the definitions of the raising and lowering operators (Sec. 3.2)

$$\mathbf{I}_x = 1/2(\mathbf{I}^+ + \mathbf{I}^-) \text{ and } \mathbf{I}_y = -i/2 (\mathbf{I}^+ - \mathbf{I}^-) \qquad (16.5.5)$$

The two-spin order represented in Cartesian coordinates can be expanded to

$$2\mathbf{I}_x\mathbf{S}_y = -i/2 [(\mathbf{I}^+ + \mathbf{I}^-) (\mathbf{S}^+ - \mathbf{S}^-)] = -i/2[\mathbf{I}^+\mathbf{S}^+ - \mathbf{I}^+\mathbf{S}^- + \mathbf{I}^-\mathbf{S}^+ - \mathbf{I}^-\mathbf{S}^-]. \qquad (16.5.6)$$

The operators with two raising or two lowering operators are double quantum states. The other terms in Eqn. 16.5.6 that have one raising and one lowering operator are zero quantum coherences. A double quantum filter extracts the $\mathbf{I}^+\mathbf{S}^+$ and the $\mathbf{I}^-\mathbf{S}^-$ terms. Pure double quantum coherence is obtained by combination of $2\mathbf{I}_x\mathbf{S}_y$ and $2\mathbf{I}_y\mathbf{S}_x$:

$$1/2i (\mathbf{I}^+\mathbf{S}^+ - \mathbf{I}^-\mathbf{S}^-) \quad = \quad (\mathbf{I}_x + i\mathbf{I}_y)(\mathbf{S}_x + i\mathbf{S}_y) - (\mathbf{I}_x - i\mathbf{I}_y)(\mathbf{S}_x - i\mathbf{S}_y), \qquad (16.5.7)$$

which is equal to

$$1/2(2\mathbf{I}_x\mathbf{S}_y + 2\mathbf{I}_y\mathbf{S}_x) \qquad (16.5.8)$$

The final 90° pulse of the mixing period, converts the double quantum state into antiphase coherence that evolves into observable magnetization during the detection period.

$$-(2\mathbf{I}_x\mathbf{S}_y + 2\mathbf{I}_y\mathbf{S}_x)\sin \pi J_{IS}t_1 \cos \omega_I t_1 \quad =\pi/2(\hat{\mathbf{I}}_x+\hat{\mathbf{S}}_x)=>$$
$$(2\mathbf{I}_x\mathbf{S}_z + 2\mathbf{I}_z\mathbf{S}_x)\sin \pi J_{IS}t_1 \cos \omega_I t_1 \qquad (16.5.9)$$

The $2\mathbf{I}_x\mathbf{S}_z$ term gives rise to a diagonal peak and the $2\mathbf{I}_z\mathbf{S}_x$ gives rise to a cross peak. Since the cross-peak signal is only collected on every other scan, the signal strength in DQFCOSY is inherently a factor of two lower than that of COSY for a spectrum collected in the same amount of time. The advantage of the DFQCOSY spectrum is that the diagonal and cross peaks are both antiphase and absorptive (See Figure 16.2.1). Any cancellation that occurs in the cross peak due to a large linewidth will also affect the diagonal peak in the same manner. The detected signals for the diagonal peak will be:

$$\mathbf{I}_y \exp(i\,\omega_I t_2)\sin \pi J_{IS}t_2 \sin \pi J_{IS}t_1 \cos \omega_I t_1 \qquad (16.5.10)$$

and for the cross peak:

$$\mathbf{S}_y \exp(i\,\omega_S t_2)\sin \pi J_{IS}t_2 \sin \pi J_{IS}t_1 \cos \omega_I t_1. \qquad (16.5.11)$$

16.5.3 DQFCOSY phase cycling:

The CTP for the DQFCOSY experiment is

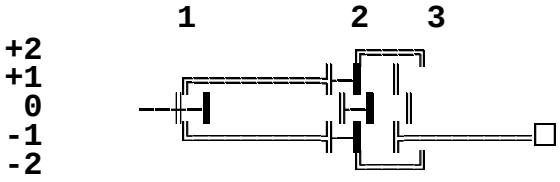

With $\Delta m_1=\pm 1$, $\Delta m_2=1,-3$, and $\Delta m_3=-3,1$ we obtain:

ϕ_1:
-1 (0 **1**)
N=2
ϕ_1 = 0,π

ϕ_2:
(**-3** -2 -1 0) 1 2 3
N=4
ϕ_2 = 0,π/2,π,3π/2

ϕ_3:
(**-3** -2 -1 0) 1 2 3
N=4
ϕ_3 = 0,π/2,π,3π/2

DQFCOSY:

ϕ_1 = 4(0 π)
ϕ_2 = 2(0) 2(π/2) 2(π) 2(3π/2)
ϕ_3 = 8(0) 8(π/2) 8(π) 8(3/2)
ψ = 0 π 3π/2 π/2 π 0 π/2 3π/2 3π/2 3π/2 π/2 π 0 π/2 3π/2 0 π
π 0 π/2 3π/2 0 π 3π/2 π/2 π/2 3π/2 0 π 3π/2 π/2 π 0

16.5.4 Variants

Multiple quantum filtering of COSY spectra is a wide ranging subject. The highest possible coherence order that
Phase Table for can be generated is equal to the number of coupled spins in the system. Filters involving higher order coherences (>2) can be used for selecting spin systems on the basis of number of spins[4] or even on the basis of the topology of the spin system[5].

One to the most used modifications of multiple quantum filtered COSY is E. COSY (Exclusive COSY)[6] or its variant P. E. COSY[7]. In E. COSY the cross peak patterns are modified by combining properly several orders of multiple quantum filtered COSY spectra. The simplification in the cross peak patterns allows for the accurate measurement of homonuclear coupling constants.

16.6 Isotropic Homonuclear Coherence Transfer

16.6.1 Total Correlation Spectroscopy (TOCSY)

Total Correlation SpectroscopY (TOCSY)[8], also known as HOmonuclear HArtmann-HAhn spectroscopy (HOHAHA)[9], has emerged in recent years to address the problem of correlating the chemical shifts of all of the spins in a scalar coupled

network. The COSY experiment transfers coherence solely between spins that have a non-zero coupling constant. In a spin system consisting of several nuclei, there may be spins that have common coupling partners but have a zero or very small coupling between them. Several modifications of COSY, *e.g.* relayed COSY and double-relayed COSY, transfer coherence from one spin to a non-coupled spin via a coupled intermediate spin. However, these experiments have characteristics that make them rather unsuitable for the correlation of spins in large molecules. The TOCSY experiment uses a mixing period consisting of a series of phase modulated 180° pulses that "trick" all of the spins into precessing at the same frequency even though each spin has a unique chemical shift. By forcing the trajectory of all spins to be cyclic within the same time period the apparent energy levels for the resonances become identical. The ultimate sequence of RF pulses would create a state of *isotropic mixing* in which energy would flow unimpeded between all of the spins that are directly or indirectly coupled. Spins that have a zero (or very small) coupling to the peaks in the spin system do not join into this orgy of energy transfer. The pulse sequence and CFN for a TOCSY experiment are shown in Figure 16.6.1.

The initial 90° pulse generates transverse magnetization at state <A>. During <A,B>, the **I** spin is frequency labeled with its chemical shift. Coupling between **I** and other spins also occurs during <A,B>; however, since inphase coherence is transferred during the mixing period, there is no essential active coupling that occurs in this period. The active coupling that does occur during <A,B> is a source of phase distortions in the cross peaks. Many sequences contain a spin-lock-trim pulse prior to the mixing period that dephases components that are orthogonal to the spin lock axis. Spin-lock-trim pulses are also used at the end of the mixing period for the same purpose. Care must be taken so that the second spin lock does not rephase components that were dephased by the first spin lock. Usually, setting different lengths for the spin lock pulses avoids this problem.

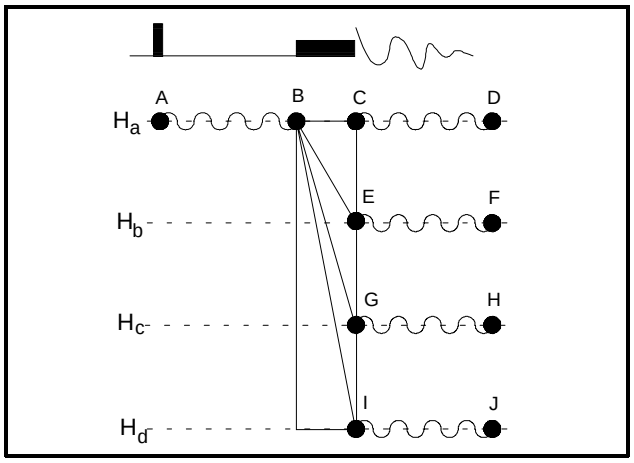

Figure 16.6.1. Pulse sequence and CFN for Total Correlation Spectroscopy (TOCSY).

An isotropic mixing sequence is applied during <B,C> that transfers coherence among all of the spins in the coupled system. The first mixing sequences that were used were borrowed from techniques for heteronuclear decoupling, such as, WALTZ and MLEV. Heteronuclear decoupling requires that the spins rotate in a cyclic manner independent of resonance offset. The splitting of the heteronucleus due to coupling is eliminated when the decoupled spins are

averaged to zero in a time frame that is small compared to the reciprocal of the heteronuclear coupling constant. The heteronuclear decoupling sequences are very good at forcing the spins into offset-independent cyclic trajectories; however, they were designed without the consideration of homonuclear coupling interactions. The TOCSY experiment relies on homonuclear coupling and the sequences do not perform as well as one might think. Newer sequences with better performance, such as DIPSI[10] and FLOPSY[11], have been designed as cyclic decoupling sequences in the presence of homonuclear coupling.

After the isotropic mixing sequence, the magnetization that started on the **I** spin is distributed throughout the spin system. Two-dimensional Fourier transformation of the time domain data yields a spectrum with cross peaks among all of the spin system components. The product operator description of the TOCSY experiment is not as simple as most other experiments, in that during the isotropic mixing period the evolution of the spin system is similar to the evolution in a strongly coupled spin system. The basis functions that comprise the normal product operator formalism are for weakly coupled systems. The main complication is that the evolution of the spins under the coupling operator no longer commutes for separate couplings involving a given spin. For example, if a spin **I** is coupled to both **S** and **T**, then during the mixing period the evolution of the **I** spin depends *simultaneously* on both J_{IS} and J_{IT}; they cannot be calculated independently. Modifications of the basis functions used in the product operator formalism can be made to correct for this problem; the methods are available in the literature.[12]
The features of TOCSY transfer can be described in a simple manner if a two-spin system is considered.[31] The evolution of coherence has the form:

$$\mathbf{I}_x = 2\pi J_{IS} t \;\; \mathbf{I}\bullet\mathbf{S} \Rightarrow 1/2 \;\; \mathbf{I}_x \{1+\cos(2\pi J_{IS} t)\} + 1/2 \;\; \mathbf{S}_x \;\; \{1+\cos(2\pi J_{IS} t)\} + (\;\; \mathbf{2I_yS_z} \;\; - \;\; \mathbf{2I_zS_y} \;) \sin(2\pi J_{IS} t) \qquad (8.1.1)$$

where $\mathbf{I}\bullet\mathbf{S}$ represents the isotropic coupling operator. Similar expressions arise for $\mathbf{I}_y$ and $\mathbf{I}_z$ components. Since the mixing is (ideally) isotropic, it occurs for transverse or longitudinal components. Antiphase components also are transferred. The noteworthy point for this type of transfer is that inphase $\mathbf{I}_x$ is transferred directly to inphase $\mathbf{S}_x$. The resulting cross-peaks are, therefore, also inphase. Although the transfer appears to "prevent the canceling" that occurs in antiphase transfer involving broad lines, the coherence transfer still relies on the coupling constant. If the spectral lines are significantly broader than the coupling constant the transfer will be quenched.

16.7. Incoherent Magnetization Transfer

16.7.1 Nuclear Overhauser Effect Spectroscopy (NOESY)

The nuclear Overhauser effect (NOE) is the feature of NMR spectroscopy that

provides for the determination of the spatial distance between two nuclei. It is this property that is the major contributor to the determination of the three dimensional structure of macromolecules in solution. Much effort has been placed in the methods to extract accurate distance information from NOESY spectra and the use of these data in the determination of three dimensional structures. A number of book and reviews cover the theory and experimental details of modern magnetization exchange spectroscopy, including NOESY, EXSY and ROESY (Rotating frame Overhauser Effect SpectroscopY).[13,14,15] Here I will discuss only the basic NOESY experiment.

The CFN for NOESY is identical to that of the EXSY (Figure 4.1.3) experiment described earlier. The transfer of magnetization by the NOE is formally identical to magnetization exchange by physical movement of the nuclei. The pulse sequence and the phase cycling are also identical between NOESY and EXSY. In a normal NOESY spectrum the exchange cross peaks are indistinguishable from the NOE cross peaks. The pulse sequence and the product operator description of NOESY are as follows:

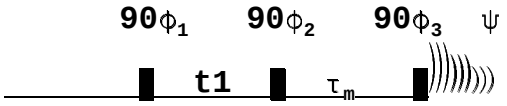

Preparation:

$$\mathbf{I}_z + \mathbf{S}_z \xrightarrow{=\pi/2\hat{\mathbf{I}}_x} -\mathbf{I}_y - \mathbf{S}_y \qquad (16.7.1)$$

Evolution:

$$\xrightarrow{=\omega_I t\hat{\mathbf{I}}_z+\omega_S t\hat{\mathbf{S}}_z} \begin{array}{l} -\mathbf{I}_y \cos\omega_I t_1 + \mathbf{I}_x \sin\omega_I t_1 \\ -\mathbf{S}_y \cos\omega_S t_1 + \mathbf{S}_x \sin\omega_S t_1 \end{array} \qquad (16.7.2)$$

Mixing :

$$\xrightarrow{=\pi/2(\hat{\mathbf{I}}_x+\hat{\mathbf{S}}_x)} \begin{array}{l} -\mathbf{I}_z \cos\omega_I t_1 + \mathbf{I}_x \sin\omega_I t_1 \\ -\mathbf{S}_z \cos\omega_S t_1 + \mathbf{S}_x \sin\omega_S t_1 \end{array} \qquad (16.7.3)$$

Applying a *zero* order coherence filter by phase cycling (Section 4.3), the state becomes

$$-\mathbf{I}_z \cos\omega_I t_1 - \mathbf{S}_z \cos\omega_S t_1. \qquad (16.7.4)$$

The system now undergoes cross relaxation according to the master equation.

$$\mathbf{M}(t) = \exp(-\mathbf{R}\tau_m)\Delta\mathbf{M}(0) \qquad (16.7.5)$$

where $\Delta\mathbf{M}(0)$ is vector containing the deviations of the magnetization from equilibrium immediately after the first 90° pulse of the mixing period and $\mathbf{M}(t)$ is the vector of magnetization after a time, τ_m, of cross relaxation. The relaxation matrix, $\mathbf{R}$, contains the auto- and cross-relaxation rate constants. During τ_m magnetization "exchanges" between the **I** and **S** nuclei. Without concerning ourselves with the details, the state at the end of the mixing period, τ_m, can be simply represented as

$$-\mathbf{I}_z (A \cos \omega_I t_1 + B \cos \omega_S t) - \mathbf{S}_z (C \cos \omega_S t_1 + D \cos \omega_I t) \qquad (16.7.6)$$

where the coefficients A through D represent amplitudes due to auto- and cross-relaxation of the spin system. In effect, some **I** magnetization has become **S** magnetization and *vice versa*. To end the mixing period a 90° pulse is applied.

$$=\pi/2(\hat{\mathbf{I}}_x+\hat{\mathbf{S}}_x)=> \quad \mathbf{I}_y (A \cos \omega_I t_1 + B \cos \omega_S t) + \mathbf{S}_y (C \cos \omega_S t_1 + D \cos \omega_I t) \qquad (16.7.7)$$

Detection:

$$=\omega_I t\hat{\mathbf{I}}_z+\omega_S t\hat{\mathbf{S}}_z=> \quad \mathbf{I}_y \exp(i\omega_I t_2) (A \cos \omega_I t_1 + B \cos \omega_S t) + \mathbf{S}_y \exp(i\omega s t_2) (C \cos \omega_S t_1 + D \cos \omega_I t) \qquad (16.7.8)$$

The detected signals, upon two-dimensional Fourier transform, yield a map of all of the spins that are close in space.

1. M. S. Friedrichs, W. J. Metzler, and L. Mueller (1991) *J. Magn. Reson.* **95**, 178.

2. A. Bax, A. F. Mehlkopf, and J. Smidt (1979) *J. Magn. Reson.* **35**, 167.

3. M. Rance, O. W. Sørensen, G. Bodenhausen, G. Wagner, R. R. Ernst, and K. Wüthrich (1983) *Biochem. Biophys. Res. Commun.* **117**, 479.

4. O. W. Sørensen, M. H. Levitt, and R. R. Ernst (1983) *J. Magn. Reson.* **55**, 104.

5. M. H. Levitt and R. R. Ernst (1985) *J. Chem. Phys.* **83**, 3306.

6. C. Griesinger, O. W. Sørensen, and R. R. Ernst (1985) *J. Am. Chem. Soc.* **107**, 6394.

7. L. Mueller (1987) *J. Magn. Reson.* **72**, 191.

8. L. Braunschweiler and R. R. Ernst (1983) *J. Magn. Reson.* **53**, 521.

9. A. Bax, D. G. Davies, and S. K. Sarkar (1985) *J. Magn. Reson.* **63**, 230.

10. A. J. Shaka, C. J. Lee, and A. Pines (1988) *J. Magn. Reson.* **77**, 274.

11. M. Kadkhodaie, O. Rivas, M. Tan, A. Mohebbi, and A. J. Shaka (1991) *J. Magn. Reson.* **91**, 437.

12. R. Bazzo and J. Boyd (1987) *J. Magn. Reson.* **75**, 452.

13. S. Macura, W. M. Westler, and J. L. Markley (1994) *Methods in Enzymology*, in press.

14. K. Wüthrich (1986) *NMR of Proteins and Nucleic Acids*, John Wiley and Sons; New York.

15. D. Neuhaus and M. Williamson (1989) *The Nuclear Overhauser Effect in Structural and Conformational Analysis*, VCH; New York.